International Journal of Power Electronics and Drive System (IJPEDS)
Vol. 4, No. 4, December 2014, pp. 499~507
ISSN: 2088-8694

Stability Analysis of DC-link Voltage Control on Autonomous Micro Hydro Power Plant System

F. Yusivar, M. Shanizal, A. Subiantoro, R. Gunawan.
Real-Time Measurement and Control Research Group, Electrical Engineering Department, Universitas Indonesia

Article Info

Article history:

Received Apr 16, 2014
Revised Jun 27, 2014
Accepted Jul 20, 2014

Keyword:

DC-link
Excitation
Micro Hydro Power Plant
Permanent Magnet-
Synchronous Machine

ABSTRACT

Micro Hydro Power Plant has become one of the interesting topics to be researched nowadays. This paper deals with the stability analysis on control system of excitation voltage in Micro Hydro Power Plant. The control of this voltage can be achieved by controlling the Permanent Magnet Synchronous Machine (PMSM) with particular algorithm so the voltage on the DC-link part of the system can be controlled. Without knowing the exact specification of system parameters, the system will be most likely unstable. The DC-link control system is modeled, simulated, and mathematically analyzed so the parameter specification for the stable system can be obtained.

Corresponding Author:

F. Yusivar
Real-Time Measurement and Control Research Group,
Electrical Engineering Department, Universitas Indonesia,
Kampus Baru UI Depok, 16424, Indonesia.
Email: yusivar@eng.ui.ac.id

1. INTRODUCTION

Micro Hydro Power Plant has been one of the most increasing uses of power generation system in the world. This type of Power Plant has high potential especially on developing country that has many rivers. The autonomous system on Micro Hydro Power Plant can be achieved by using Doubly Fed Induction Generator (DFIG) and Permanent Magnet Synchronous Machine (PMSM). Block diagram of the system is shown in Figure 1.

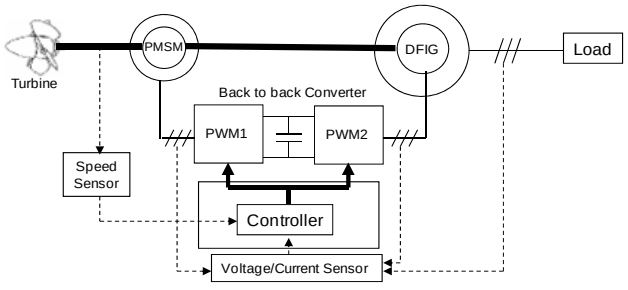

Figure 1. Microhydro DFIG generation system with PMSM exitation.

The system shown in Figure 1 can be divided into two independent control systems. The first system is regulating the stator voltage to load by controlling DFIG and the second system is regulating the excitation

voltage by controlling PMSM. On this study, we are focusing on the control of excitation voltage on the system. Therefore the second system is mainly used for easier analysis that will be performed in this paper. The simplified system can be done by replacing the excitation load (DFIG) system by pure resistive load. Figure 2 shows the simplified system that is used in this study.

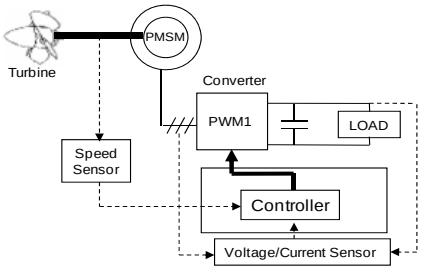

Figure 2. Simplified system scheme

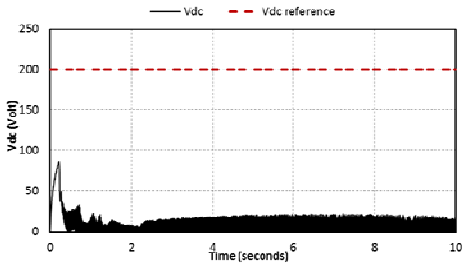

Figure 3. Stability problem in the excitation voltage (V_{dc}) system of Autonomous Micro Hydro Power Plant

Stability problem arise in the excitation voltage control system without using an appropriate value of parameters such as water velocity, voltage reference, load resistance, etc. For example, Figure 3 shows the excitation voltage (DC-link voltage) result when a simulation is performed with random value of mentioned parameters. The simulation is performed by using MATLAB's Simulink.

From simulation result shown on Figure 3, it is noticed that unstable system condition could occur if an inappropriate value of certain parameters is used. To clarify this issue, it is necessarry to examine this control problem deeply. The system is modeled and then simulated and analyzed mathematically in order to know the exact value of those parameters. By using this method, the parameter's value required to achieve stable system can be noticed.

2. SYSTEM MODEL

The whole system is composed of PMSM, shafts, turbine, inverter, DC-link, and controller. Each one of these components is mathematically modeled to ease the analysis process.

2.1. PMSM Model

Electrical model of PMSM is expressed by (1) and (2).

$$\frac{d}{dt}i_d = \frac{1}{L_d}v_d - \frac{R_s}{L_d}i_d + \frac{L_q}{L_d}p\omega_r i_q \quad (1)$$

$$\frac{d}{dt}i_q = \frac{1}{L_q}v_q - \frac{R_s}{L_q}i_q - \frac{L_d}{L_q}p\omega_r i_d - \frac{\varphi p\omega_r}{L_q} \quad (2)$$

Where p is pole pairs, ω_r rotor speed, R_s stator resistance, L_d and L_q the direct and quadrature axis inductances, $v_d, v_q, i_d, i_q$are the direct and quadrature axis voltage and current components, and φ is the permanent magnet flux.

Mechanical model of PMSM will be discussed on shaft subsection because the state (rotor speed) on PMSM is the same as rotating speed of the shaft.

2.2. Shaft Model

Differential equation of the shaft is expressed as:

$$\frac{d}{dt}\omega_r = (-B\omega_g + T_e - \frac{T_m}{K}) / (\frac{J_m}{K^2} + J_p) \quad (3)$$

$$T_e = p\varphi i_q \quad (4)$$

Where B is internal damping, T_e is electrical torque from PMSM, T_m is mechanical torque from turbine, K is gear ratio, J_m and J_p are inertia of turbine and PMSM.

2.3. Turbine Model

Turbine component does not have its own state. This component just continuing rotor speed's feedback state from shaft and water velocity from its input. Output of this component is mechanical torque to shaft as expressed in (5).

$$T_m = -\frac{0.5\,\rho\, c_p\, s\, {v_w}^3}{\omega_r} \quad (5)$$

Where ρ is water density, s is turbine swept, v_w is water velocity, and c_p is turbine constant.

2.4. Inverter Model

The inverter is assumed as an ideal power conversion machine with an efficiency factor η. The power conversion expression of inverter model for analysis purpose is expressed as:

$$\eta \mathrm{V}_{dc} i_{in} = \mathrm{v_d i_d} + \mathrm{v_q i_q} \quad (6)$$

In the analysis the inverter is assumed to be ideally efficient, therefore η = 1.

The only state in this component is DC voltage detection of inverter which can be expressed as:

$$\frac{\mathrm{d}}{\mathrm{dt}} \mathrm{V}_{dc\,det} = -\frac{1}{\mathrm{T_{DC}}} \mathrm{V}_{dc\,det} + \frac{1}{\mathrm{T_{DC}}} \mathrm{V}_{dc} \quad (7)$$

Where $\mathrm{V}_{dc\,det}$ is DC voltage detection value, $\mathrm{T_{DC}}$ is detection time constant, and V_{dc} is DC-link voltage.

2.5. DC-link Model

DC-link circuit structure can be seen on Figure 2. Modeling of this circuit can be done by using basic Kirchhoff's law and can be expressed as:

$$\frac{d}{dt} V_{dc} = \frac{i_{in}}{C} - \frac{v_{dc}}{CR} \quad (8)$$

Where i_{in} is input current on DC-link circuit, C is capacitor's capacitance, and R is load's resistance.

2.6. Controller Model

The algorithm and modeling of this controller is expressed by the state equations as follows:

$$\frac{d}{dt} x_d = i_d^* - i_d \quad (9)$$

$$\frac{d}{dt} x_q = i_q^* - i_q \quad (10)$$

$$\frac{d}{dt} i_{d1}^* = \frac{1}{T_d} i_d^* - \frac{1}{T_d} i_{d1}^* \quad (11)$$

$$\frac{d}{dt} i_{q1}^* = \frac{1}{T_d} i_q^* - \frac{1}{T_d} i_{q1}^* \quad (12)$$

$$\frac{d}{dt} x_{dc} = v_{dc}^* - v_{dc} \quad (13)$$

$$i_d^* = 0 \quad (14)$$

$$i_q^* = -k_{pdc} v_{dc} + k_{idc} x_{dc} \quad (15)$$

Where T_d is controller's time constant, k_{pdc} and k_{idc} are DC-voltage controller constants.

3. RESULTS AND ANALYSIS

Simulation method used in this study is to do a variation of several parameters: water velocity, DC voltage reference, resistive load, and controller constant. Variation is performed by changing one of the parameter as independent variable while keeping others with there initial value. The system is simulated in Matlab and the result is obtained and analyzed graphically and mathematically. Model's parameter is shown in Table 1 and some variable values are initially stated as shown on Table 2.

Table 1. System Parameters

Parameter	Symbol	Value
PMSM inertia	J_p	0,01 $[kgm^2]$
Turbine inertia	J_m	0,5 $[kgm^2]$
Shaft Internal Damping	B	0,001 [Nms]
Gear ratio	K	9
Stator Resistance	R_s	0,55 [Ω]
Direct axis inductance	L_d	16,61 [mF]
Quadrature axis inductance	L_q	16,61 [mF]
Permanent magnet flux	φ	0.121 [Wb]
Pole pairs	p	4
Controller time constant	T_d	10 [ms]
DC-voltage detection time constant	T_{DC}	100 [ms]
DC-link capacitance	C	0.1 [mF]

Table 2. Initially Stated Variables Value

Parameter	Symbol	Value
Water velocity	v_w	2 $[m/s]$
DC-voltage reference	V_{dc}^*	60 [V]
DC-voltage controller proportional constant	k_{pdc}	0,3
DC-voltage controller integral constant	k_{idc}	0,7
Load resistance	R	1000 [Ω]

System stability is reviewed through poles location of the linearized system which is described by state equation and expressed in Appendix. State variables of the linearized system are as follows:

$$x = [\Delta V_{dc} \quad \Delta i_d \quad \Delta i_q \quad \Delta x_{dc} \quad \Delta x_d \quad \Delta x_q \quad \Delta i_{d1}^* \quad \Delta i_{q1}^* \quad \Delta V_{dc\,det} \quad \Delta \omega_r]^T \tag{16}$$

The result of the system that has initially stated parameters is shown in Figure 4. It shows that when the parameters used on the system equal to the value that was shown on Table 2, the system is stable. Thus these parameters are used as base variables. One of these parameter will be variated for analysis purpose.

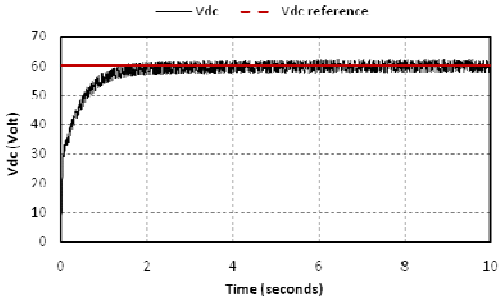

Figure 4. DC-link voltage when $V_{dc}^* = 60\ V$

3.1. DC-Voltage Reference Variation

Simulation results can be seen on Figure 5. Results show that the system can withstand in a certain range of DC voltage reference. On this occasion, if DC voltage reference value is not between 20 and 100 volt, the system will be unstable. To describe this situation, poles location of each system is derived as shown

in Table 3. It is clearly noticed that there is an unstable pole which is located in the Righ Half Plane (RHP) if the DC-voltage reference is out of its certain range.

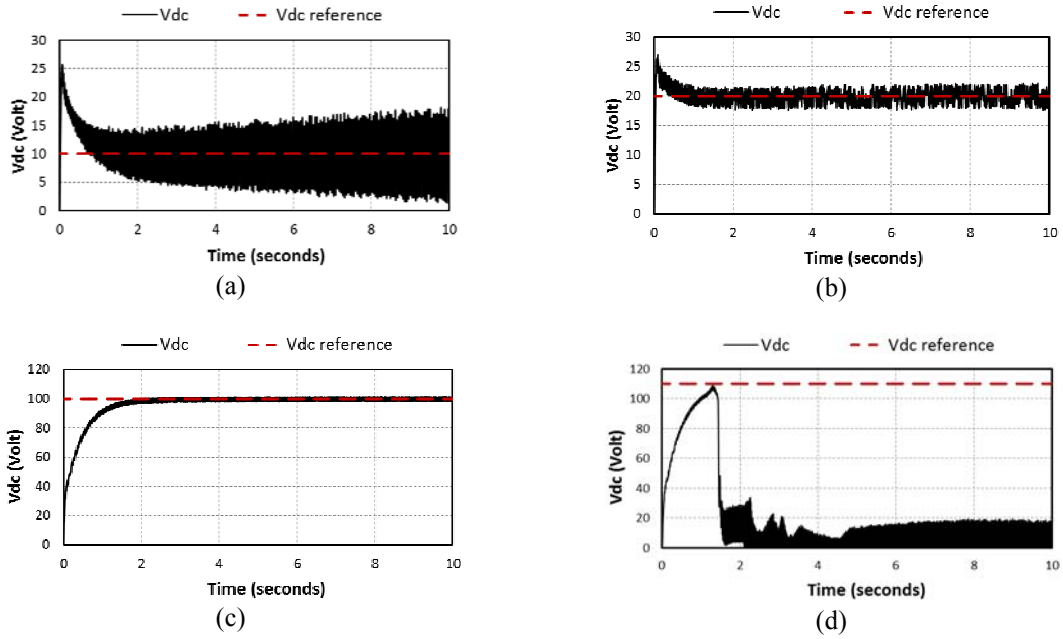

Figure 5. Simulation results when: (a) $\boldsymbol{V_{dc}^{*} = 10\ V}$, (b) $\boldsymbol{V_{dc}^{*} = 20\ V}$, (c) $\boldsymbol{V_{dc}^{*} = 100\ V}$, (d) $\boldsymbol{V_{dc}^{*} = 110\ V}$

Table 3. Poles Location to V_{dc}^{*} Variations

Poles	V_{dc}^{*}(Volt)			
	10	20	100	110
Pole 1	7.43 - 30.66i	-0.19 + 0.12i	- 0.28 + 0.24i	- 0.07 - 0.17i
Pole 2	7.43 + 30.66i	-0.19 - 0.12i	- 0.28 - 0.24i	- 0.07 + 0.17i
Pole 3	-0.394	-22.402	-21.081	40.767
Pole 4	-0.452	-0.457	-0.463	-0.730
Pole 5	-9.661	-9.415	-9.937	-9.362
Pole 6	- 16.27 + 15.07i	-40.578	- 66.74 + 20.08i	- 34.36 + 141.82i
Pole 7	- 16.27 - 15.07i	-91.120	- 66.74 - 20.08i	- 34.36 - 141.82i
Pole 8	-52.920	-177.375	-115.95 - 108.07i	- 198.28 - 126.65i
Pole 9	-87.349	-749.216	-115.95 + 108.07i	- 198.28 + 126.65i
Pole 10	-100.000	-100.000	-100.000	-100.000

3.2. Water Velocity Variation

Simulation results can be seen in Figure 6 and poles locations are shown in Table 4. Results show that system tends to be stable if high water velocity occurred. Low water velocity can cause the system to become unstable. This problem can be resolved by readjusting the given reference voltage to lower value.

Table 4. Poles Location to v_w Variations

Poles	Water Velocity (m/s)			
	1	1.5	2.5	3
Pole 1	-0.33 + 0.17i	-0.38 + 0.20i	-0.22 - 0.19i	-0.19 + 0.20i
Pole 2	-0.33 - 0.17i	-0.38 - 0.20i	-0.22 + 0.19i	-0.19 - 0.20i
Pole 3	-38.316	-13.933	-20.888	-23.534
Pole 4	-3.654	-0.540	-0.342	-0.265
Pole 5	-9.228	-10.159	-9.727	-9.559
Pole 6	12.162	-43.945	-58.791	-64.24 + 26.43i
Pole 7	51.185	-91.388	-72.713	-64.24 - 26.43i
Pole 8	-76.54 + 29.78i	-87.86 - 80.23i	-154.48 - 101.33i	-190.59 + 92.14i
Pole 9	-76.54 - 29.78i	-87.86 + 80.23i	-154.48 + 101.33i	-190.59 - 92.14i
Pole 10	-100.000	-100.000	-100.000	-100.000

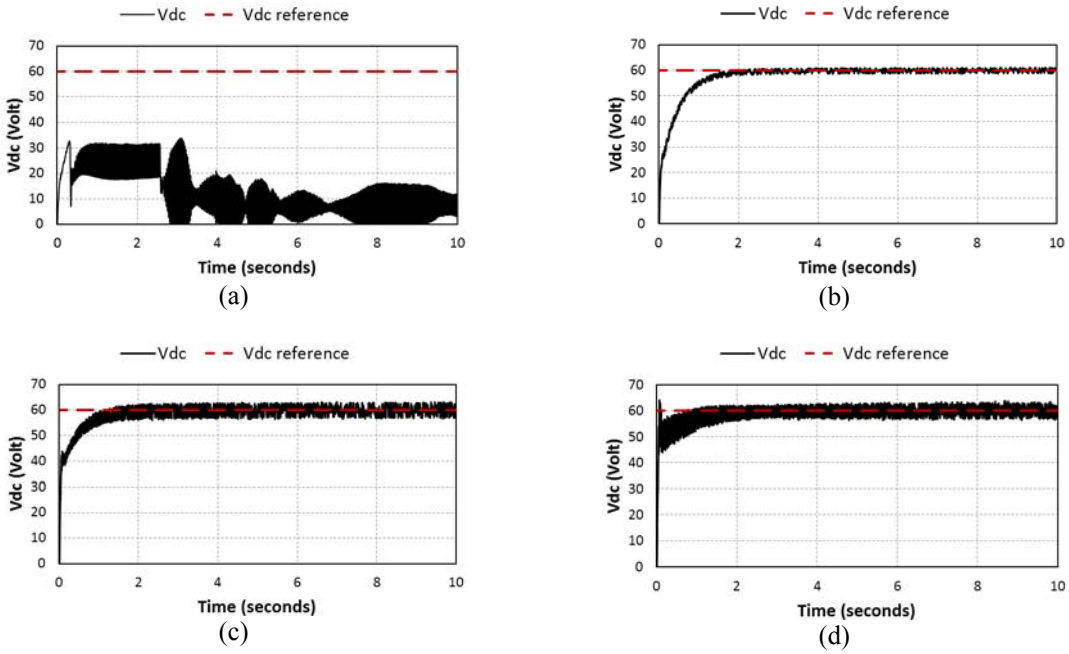

Figure 6. Simulation results when: (a) $\mathbf{v_w = 1\ m/s}$, (b) $\mathbf{v_w = 1.5\ m/s}$, (c) $\mathbf{v_w = 2.5\ m/s}$, (d) $\mathbf{v_w = 3\ m/s}$

3.3. Load Resistance Variation

Simulation results can be seen on Figure 7 and poles locations are shown in Table 5. Results show that system tends to be unstable if the load resistance is small. The system is relatively stable if high load resistance is implemented.

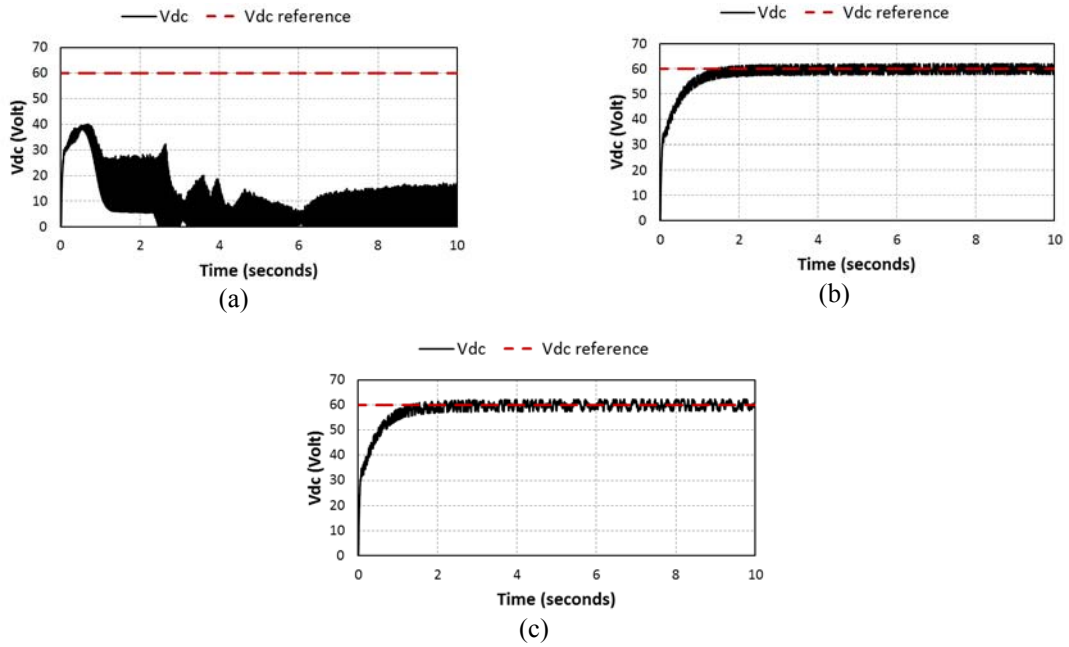

Figure 7. Simulation results when: (a) R = 100 Ω, (b) R = 1000 Ω, (c) R = 10000 Ω

Table 5. Poles Location to R Variations

Poles	R (Ohm)		
	100	1000	10000
Pole 1	- 0.192 + 0.195 i	- 0.238 + 0.18 i	- 0.259 + 0.196 i
Pole 2	- 0.192 - 0.195 i	- 0.238 - 0.18 i	- 0.259 - 0.196 i
Pole 3	7.224	-19.894	-16.808
Pole 4	0.466	-0.443	-0.441
Pole 5	-9.957	-9.840	-9.804
Pole 6	- 59.804 + 81.537 i	-45.435	-42.572
Pole 7	- 59.804 - 81.537 i	-87.951	-91.135
Pole 8	- 195.408 + 100.285 i	- 174.271 + 108.708 i	- 124.21 - 95.38 i
Pole 9	- 195.408 - 100.285 i	- 174.271 - 108.708 i	- 124.21 + 95.38 i
Pole 10	-100.000	-100.000	-100.000

3.4. Controller Constant Variations

Simulation result can be seen on Figure 8 and poles locations are shown in Table 6. Results show that controller constant does not much affect the system stability as long as within the acceptable range. Controller constant only affect system response characteristics.

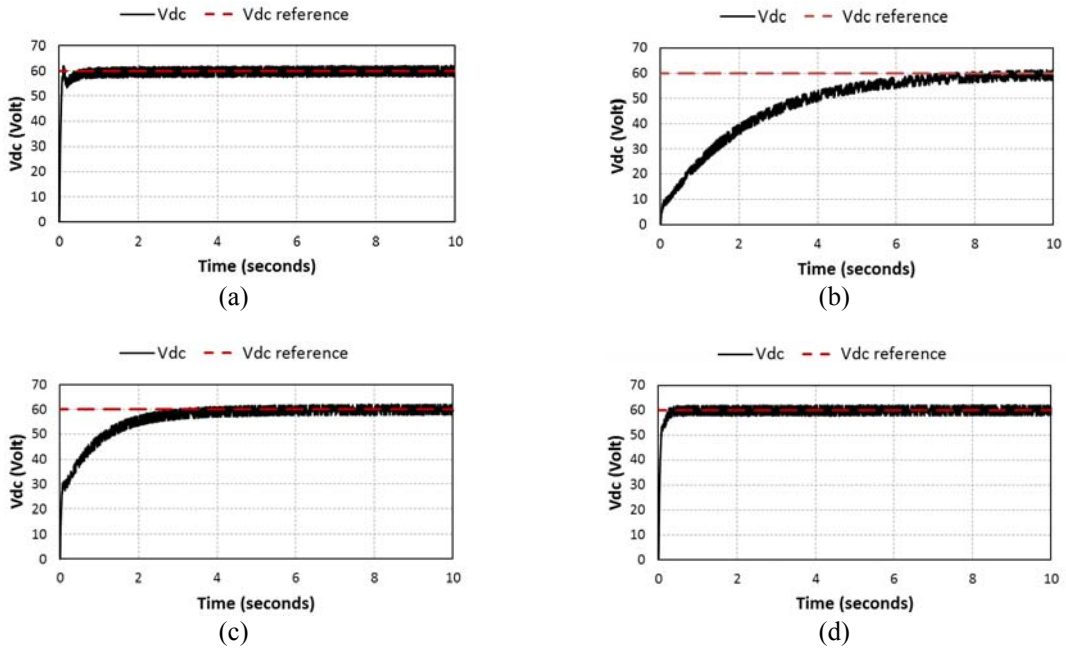

Figure 8. Simulation results when: (a)$k_{pdc} = 0.15$, (b) $k_{pdc} = 1.5$, (c) $k_{idc} = 0.35$, (d) $k_{idc} = 3.5$

Table 6. Poles Location to k_{pdc} and k_{idc} Variations

Poles	Proportional Constant Variation		Integral Constant Variation	
	k_{pdc}=0.15, k_{idc}=0.7	k_{pdc}=0.5, k_{idc}=0.7	k_{pdc}=0.3, k_{idc}=0.35	k_{pdc}=0.3, k_{idc}=3.5
Pole 1	- 0.326 + 0.239 i	-0.07	- 0.191 + 0.089 i	- 0.442 + 0.137 i
Pole 2	- 0.326 - 0.239 i	-0.262	- 0.191 - 0.089 i	- 0.442 - 0.137 i
Pole 3	-19.619	-19.598	-19.89	-17.068
Pole 4	-0.477	-0.413	-0.425	-1.075
Pole 5	-9.808	-9.983	-9.915	-9.859
Pole 6	-45.512	-45.314	-45.386	-45.359
Pole 7	-87.046	-88.887	-88.219	-88.277
Pole 8	- 88.231 + 64.441 i	-212.391	- 120.976 + 96.613 i	- 121.823 - 89.961 i
Pole 9	- 88.231 - 64.441 i	-561.979	- 120.976 - 96.613 i	- 121.823 + 89.961 i
Pole 10	-100	-100	-100	-100

4. CONCLUSION

There is a stability problem on the Autonomous Micro Hydro Power Plant system caused by low water velocity, out of range DC voltage reference, and low load resistance. In this paper, for 2m/s water

velocity, the parameters required to achieve stable system are DC-voltage reference of 20-100 Volt and load resistance of 1000-10000 Ohm. If the water velocity is lower, then readjustment to lower voltage reference is required. The controller constant does not affect system stability as long as within acceptable range. Prospect for further study is adding Doubly Fed Induction Generator (DFIG) to the system so the overall Micro Hydro Power Plant system is completed.

ACKNOWLEDGEMENTS

This work was partially funded by the Universitas Indonesia under international collaboration grant with contract number: 0684/H2.R12/HKP.05.00 Perjanjian/2013. The authors would like to thank Prof. Tian-Hua Liu, researcher at National Taiwan University of Science and Technology as our collaboration partner.

REFERENCES

[1] F Khatounian, E Monmasson, F Berthereau, E Delaleau, JP Louis. Control of a Doubly Fed Induction Generator for Aircraft Application. Industrial Electronics Society. 2003; 1: 2711-2716.
[2] Nababan S,Muljadi E, Blaabjerg F. *An overview of power topologies for micro-hydro turbines.* IEEE International Symposium on Power Electronics for Distributed Generation Systems (PEDG), 2012 , Page(s): 737 – 744.
[3] Andreica M, Bacha S, Roye D, Exteberria-Otadui I, Munteanu I. *Micro-hydro water current turbine control for grid connected or islanding operation*. IEEE Power Electronics Specialists Conference, 2008. PESC 2008. Page(s): 957 – 962.
[4] Breban S, Nasser M, Vergnol A, Robyns B, Radulescu MM. *Hybrid wind/microhydro power system associated with a supercapacitor energy storage device - experimental results*. 18th International Conference on Electrical Machines, 2008. ICEM. 2008: 1-6.
[5] Breban S, Robyns B, Radulescu MM. *Study of a grid-connected hybrid wind/micro-hydro power system associated with a supercapacitor energy storage device.* 12th International Conference on Optimization of Electrical and Electronic Equipment (OPTIM). 2010: 1198 – 1203.
[6] Faria J, Margato E, Resende MJ. *Self-Excited Induction Generator for Micro-Hydro Plants Using Water Current Turbines Type.* Twenty-Seventh International Telecommunications Conference. INTELEC '05. 2005: 107 – 112.
[7] Breban S, Robyns B, Radulescu MM. Islanding detection methods for a micro-hydro power station - Simulation and experimental results. 8th International Symposium on Advanced Electromechanical Motion Systems & Electric Drives Joint Symposium, *ELECTROMOTION* 2009: 1 – 6.
[8] Scherer LG, de Camargo RF. *Control of micro hydro power stations using nonlinear model of hydraulic turbine applied on microgrid systems.* Brazilian Power Electronics Conference (COBEP), 2011: 812 – 818.
[9] Scherer LG, de Camargo RF. *Frequency and voltage control of micro hydro power stations based on hydraulic turbine's linear model applied on induction generators.* Brazilian Power Electronics Conference (COBEP), 2011: 546 – 552.
[10] Guocheng Wang, Qingzhi Zhai, Jianhua Yang. *Voltage control of cage induction generator in micro hydro based on variable excitation*. International Conference on Electrical Machines and Systems (ICEMS). 2011: 1 – 3.

APPENDIX

Linearized System:

$$\frac{d}{dt}\begin{bmatrix} \Delta V_{dc} \\ \Delta i_d \\ \Delta i_q \\ \Delta x_{DC} \\ \Delta x_d \\ \Delta x_q \\ \Delta i_{d1}^* \\ \Delta i_{q1}^* \\ \Delta V_{dcdet} \\ \Delta \omega_r \end{bmatrix} = \begin{bmatrix} Y_{11} & Y_{12} & Y_{13} & Y_{14} & 0 & Y_{16} & Y_{17} & 0 & Y_{19} & Y_{110} \\ Y_{21} & Y_{22} & Y_{23} & 0 & Y_{25} & 0 & 0 & Y_{28} & Y_{29} & 0 \\ Y_{31} & Y_{32} & Y_{33} & Y_{34} & 0 & Y_{36} & Y_{37} & 0 & Y_{39} & 0 \\ -1 & 0 & 0 & 0 & 0 & 0 & 0 & 0 & 0 & 0 \\ 0 & -1 & 0 & 0 & 0 & 0 & 0 & 0 & 0 & 0 \\ -k_{pdc} & 0 & -1 & k_{idc} & 0 & 0 & 0 & 0 & 0 & 0 \\ 0 & 0 & 0 & 0 & 0 & 0 & \frac{-1}{T_d} & 0 & 0 & 0 \\ \frac{-k_{pdc}}{T_d} & 0 & 0 & \frac{k_{idc}}{T_d} & 0 & 0 & 0 & \frac{-1}{T_d} & 0 & 0 \\ \frac{1}{T_{dc}} & 0 & 0 & 0 & 0 & 0 & 0 & 0 & \frac{-1}{T_{dc}} & 0 \\ 0 & 0 & Y_{103} & 0 & 0 & 0 & 0 & 0 & 0 & T_{m0} \end{bmatrix} \begin{bmatrix} \Delta V_{dc} \\ \Delta i_d \\ \Delta i_q \\ \Delta x_{dc} \\ \Delta x_d \\ \Delta x_q \\ \Delta i_{d1}^* \\ \Delta i_{q1}^* \\ \Delta V_{dcdet} \\ \Delta \omega_r \end{bmatrix}$$

Where:

$Y_{11} = \frac{i_{q0}.v_{q0}}{C.V_{dc0}^2} - \frac{i_{q0}.k_{pq}.k_{pdc}}{C.V_{dc0}} - \frac{i_{in0}}{C.V_{dc0}} - \frac{1}{C.R}$; $Y_{12} = \frac{v_{d0}}{C.V_{dc0}}$; $Y_{13} = \frac{V_{q0} - i_{q0}.k_{pq}}{C.V_{dc0}}$; $Y_{14} = \frac{i_{q0}.k_{pq}.k_{idc}}{C.V_{dc0}}$; $Y_{16} = \frac{i_{q0}.k_{iq}}{C.V_{dc0}}$; $Y_{17} = \frac{i_{q0}.p.\omega_{r0}.L_d}{C.V_{dc0}}$; $Y_{19} = -\frac{i_{q0}.v_{q0}}{C.V_{dc0}^2}$; $Y_{110} = \frac{i_{q0}.p.\varphi}{C.V_{dc0}}$; $Y_{21} = \frac{v_{d0}}{V_{dc0}.L_d}$; $Y_{22} = \frac{R_S - k_{pd}}{L_d}$; $Y_{23} = \frac{L_q.p.\omega_{r0}}{L_d}$; $Y_{25} = \frac{k_{id}}{L_d}$; $Y_{28} = -\frac{L_q.p.\omega_{r0}}{L_d}$; $Y_{29} = -\frac{v_{d0}}{V_{dc0}.L_d}$; $Y_{31} = \frac{v_{q0}}{V_{dc0}.L_q} - \frac{k_{pq}.k_{pdc}}{L_q}$; $Y_{32} = -\frac{L_d.p.\omega_{r0}}{L_q}$; $Y_{33} = \frac{-R_S - k_{pq}}{L_q}$; $Y_{34} = \frac{k_{pq}.k_{idc}}{L_q}$; $Y_{36} = \frac{k_{iq}}{L_q}$; $Y_{37} = \frac{L_d.p.\omega_{r0}}{L_q}$; $Y_{39} = -\frac{v_{q0}}{V_{dc0}.L_q}$; $Y_{103} = p.\varphi$

BIOGRAPHIES OF AUTHORS

Feri Yusivar was born in Bandung, Indonesia. He received his Bachelor degree in Electrical Engineering at Universitas Indonesia in 1992, and completed his Doctor degree in 2003 at Waseda University, Japan. He is currently the Head of Control Laboratory in Electrical Engineering at Universitas Indonesia. His research interests are control system, electrical drive, power electronics, and renewable energy.

M. Shanizal Hasny was born in Jakarta, Indonesia in 1992. He is currently pursuing bachelor degree in Electrical Engineering at Universitas Indonesia. His areas of interests involve control systems and electrical machines.

Aries Subiantoro was born in Jakarta, Indonesia. He received his Bachelor degree in Electrical Engineering at Universitas Indonesia in 1995, and completed his Doctor degree in 2013 at Universitas Indonesia. His research interests are model and simulation, intelligent control system, and model predictive control system.

Ridwan Gunawan was born in Jakarta, Indonesia. He received his Bachelor degree in Electrical Engineering at Universitas Indonesia in 1978, and completed his Doctor degree in 2006 at Universitas Indonesia. His research interests are power system, electrical drive system, and power electronics system.